



Modification of polymer thin film-coated metallic layer inside acid solutions

SUMAN SARKAR^{1,2}, BIJAY KUMAR SAH^{1,3} and SARATHI KUNDU^{1,*} 

¹Soft Nano Laboratory, Physical Sciences Division, Institute of Advanced Study in Science and Technology, Guwahati 781035, India

²Present Address: Physics Department, Gossaigaon College, Kokrajhar 783360, India

³Present Address: Department of Physics, Goalpara College, Goalpara 783101, India

*Author for correspondence (sarathi.kundu@gmail.com)

MS received 1 September 2020; accepted 22 November 2020

Abstract. Modification of polystyrene (PS) thin film-coated copper (Cu) layer is studied by varying the PS layer thickness inside different acidic environments. PS-coated Cu films are exposed to acetic and hydrochloric acid environments and are investigated using UV–visible spectroscopy, atomic force microscopy, water contact angle and electrical measurements. Polymeric and metallic layer thicknesses are obtained from the X-ray reflectivity analysis. It is found that the metallic layer corrosion nearly follows an exponential decay with time and the decay time constant takes the higher values for the thicker PS films. The contact angle values, surface morphologies and in-plane current–voltage curves obtained from the films confirm that with increase in the acid concentration, corrosion of the metallic layer is much higher than the polymeric layer, as the in-plane current is reduced by a relatively higher value than the water contact angle. Penetration of the acid solution through intermolecular spacing or microscopic pores of the polymeric layer is the most probable reason for such corrosion of the metallic layer, but the removal of the polymeric layer is not favourable due to the hydrophobic effect.

Keywords. Metallic layer corrosion; polymer coating; acid solutions; UV–vis spectroscopy; water contact angle; current–voltage curves.

1. Introduction

Metals such as copper, aluminium, zinc, iron, etc. show excellent physical, mechanical and physicochemical properties and therefore are widely used in our daily life, including different fields of scientific and industrial applications. These metals highly react with water and oxygen and therefore, in the ambient conditions, the surfaces of such metals are oxidized and change its metallic behaviours. This reaction significantly affects the mechanical, electrical and optical properties of the metals. Such oxidation subsequently decreases the lifetime of such metallic substances and even causes several damages, which may cause an extensive economic loss [1,2].

Metals can be protected from corrosion most effectively and economically in environmental adversity using coatings. Coatings generally protect such metals by forming a thin layer over its surface. There are different experimental methods to develop different types of organic and inorganic coatings [3]. The organic coating is a type of paint having a polymeric compound as the main ingredient, and after drying, it acts as a hard thin layer over the metallic substrates [4]. Therefore, when coated over the metal surfaces, depending upon the intrinsic properties,

such an organic coating layer can effectively prevent the effects of the outside environment's unfavourable medium and provide an effective improvement on metal durability. As an alternative to inorganic coatings, organic coatings can provide better efficiency as it is cost effective [5]. Specific organic thin films like self-assembled monolayers (SAM), Langmuir–Blodgett (LB) films, spin-coated and dip-coated films, etc. are used as a protective metal layer against corrosion and biofouling [6]. Coating from different compounds such as thiols [7–21], thiosulphates [20], carboxylic acids [22–28], hydroxamic acids [28–30], amino acids [31–33], phosphonic acids [28,34], etc. have proven themselves effective against corrosion [34]. In the oil and gas industries, some short-chain organic acids, such as formic acid (CHOOH), acetic acid (CH₃COOH), propionic acid (CH₃CH₂COOH), etc. are commonly encountered, which are mainly responsible for the corrosion of the metals and alloys [35–38]. Among all the organic acids, acetic acid is the most abundant species. Therefore, in corrosion studies, acetic acid has been commonly used to represent the effects of all organic acids [35]. On the other hand, in the industry for pickling, chemical and electrochemical etching of metals, hydrochloric acid (HCl) solutions are commonly used [39]. Due to the formation of an amphoteric layer over the metal surfaces, corrosion occurs when

immersed in the HCl solution. Like organic coating layers, different organic inhibitors are also used to reduce metals corrosion in the acidic medium [39,40]. However, it is evident that by exposure to sunlight, heat, water, salt, alkaline or acidic environments, the materials quality and the protective effect degrade gradually [41–44]. Out of so many possibilities of organic-coating layers, polymeric materials are used as a coating layer because it is extensively available, inexpensive and non-biodegradable. Moreover, it is well soluble in some common and inexpensive solvents [45]. Although different studies are available on the coating nature of polymeric thin films, a systematic study on the variation of structures, morphology and properties of polymeric thin film coated as a protective metallic layer in the presence of different acidic environments is not explored properly.

In this article, polystyrene (PS) film is deposited on the copper (Cu) layer and their surface modifications are studied in the presence of acetic and hydrochloric acid environments. Using spin coating method, thin films of PS of various thicknesses are deposited on Cu surface, while DC magnetron sputtering method is used to deposit Cu layers on glass substrates. In ambient conditions, a thin layer of copper oxide (CuO) is always present on the Cu surface. These PS-coated Cu films are then dipped inside aqueous solutions of acetic and hydrochloric acids of different concentrations. Thicknesses of both organic and metallic layers are obtained from the X-ray reflectivity analysis. Corrosion of Cu/CuO layer with time inside acid solutions is obtained from the results of UV–visible absorptions. Surface morphology and hydrophobic nature of the films before and after interaction with the acid solutions for a reasonable time are obtained from the atomic force microscopy and water contact angle measurements. In addition, the electrical behaviours of the Cu films before and after interaction with the acids are also studied from the current–voltage (I – V) curves. It is found from the UV–visible analysis that the corrosion of the metallic layer nearly follows an exponential decay with time, and the decay time constant (τ) takes the higher values for the thicker PS films. The water contact angle and the in-plane current of the PS-coated Cu layer decreases after dipping inside the acid solutions. It happens as PS-coated Cu layer is partially detached from the glass surface, which is also visible from the variation of the surface morphology. However, with increase in acid concentration, the corrosion of metallic layer is much higher than the polymeric layer, as the decrement in the in-plane current is higher than the water contact angle. Surface modifications and the reason for such different organic and metallic corrosions are also proposed.

2. Experimental

Copper films over the glass substrates were prepared inside a vacuum chamber by DC magnetron sputtering technique designed by Excel Instruments, India. Before Cu deposition,

cleaning of the glass substrates was done by boiling them in a mixture of ammonium hydroxide (NH₄OH, Merck, 30%), hydrogen peroxide (H₂O₂, Merck, 30%) and Milli-Q water in a ratio of H₂O:NH₄OH:H₂O₂ = 2:1:1, by volume for 5–10 min at 100°C and then drying them at room temperature (24°C). The dimensions of the glass substrates used in this study were ≈ 20.0 mm \times 12.0 mm \times 1.0 mm. A Cu target used in DC magnetron sputtering has a diameter of 5 cm and thickness of 2.5 mm. The substrate holder was kept at a constant distance of ≈ 6 cm from the target. Initially, the chamber was evacuated to 1.5×10^{-6} Torr by using turbo molecular pump backed by a rotary pump. During the deposition, argon gas (purity 99.99%) was used in the vacuum chamber at a constant flow rate (20 sccm) and the chamber pressure was maintained at 1.5×10^{-2} Torr and in between the electrodes, voltage difference of 0.33 kV and current of 1.6 A was applied. Before exposing the substrates to the sputtered atoms (in the form of plasma), the Cu target was pre-sputtered so that any kind of impurities can be removed from the surface of it. The Cu deposition over the glass substrate was carried out for 5 min and the Cu covered glass substrate is designated as Glass-Cu.

After collecting the Glass-Cu films, PS ($M_w \approx 524$ kg mol⁻¹, Sigma Aldrich, Cat. no. 81415-1G) layer was deposited on top of the Cu surface using spin coating method. The PS thin films were deposited over Glass-Cu films by spreading the desired amount (~ 200 μ l) of PS solution (concentration: 10 mg ml⁻¹) on the substrates and then spin coating at three different rotational speeds of 3000, 6000 and 9000 rpm, respectively, by using spin-coater (Apex Spin XNG-P2). PS layer coated on Glass-Cu films were designated as Glass-Cu-PS3000, Glass-Cu-PS6000 and Glass-Cu-PS9000, respectively, and all the films are left overnight at room temperature (24°C) for drying.

After drying, films were dipped inside acetic acid (CH₃COOH, Merck, 99.9%) and hydrochloric acid (HCl, Merck, 35%) solutions of different concentrations. For acetic acid, solutions of three different concentrations, i.e., 1.0, 2.5 and 10.0 vol% were chosen, whereas for hydrochloric acid solutions, the chosen concentrations were 0.1, 0.15 and 0.2 vol%. Specific acid concentrations were selected depending upon the limiting information obtained from the UV–visible absorbance values. During the PS layer preparation, a sufficient amount of PS solution was taken. Therefore, it overflows the substrate and subsequently covers the side portions of the Cu layer. Thus, the obtained variation in metallic corrosion is due to acid penetration through the front side only. In this study, three different acid concentrations were chosen to see the effects of the concentration variation of acids on PS-coated Cu layers corrosion. UV–visible absorption spectra were taken from the film following some regular interval of time up to a specific dipping time. For UV–visible absorption spectra, a Shimadzu UV-1800 spectrophotometer was used [46]. In-plane electrical behaviours of each Glass-Cu-PS film before and after dipping inside the acid solutions was obtained by

performing electrical measurements using van der Pauw (VDP) four-probe method with DC source meter (Keithley 2635B). Before measurements, four electrodes were prepared at 10 mm apart using silver paste and were connected with DC source metre using copper wires and clips. To study the variation in hydrophobicity of the Glass-Cu-PS film surfaces, before and after interaction with the acid solutions, water contact angle measurements were performed. For getting information about film thickness, X-ray reflectivity (XRR) measurements were carried out using an X-ray diffractometer (D8 Advanced, Bruker AXS) having a copper (Cu) source in a sealed tube followed by a Göbel mirror for the selection and enhancement of the Cu K_α radiation ($= 1.54 \text{ \AA}$). The scattered beam was collected using NaI scintillation detector in a specular condition, i.e., the incident and reflected angle (θ) were same and both lying in the same scattering plane. Under these conditions, there exists a wave vector component $q_z = (4\pi/\lambda) \sin\theta$ normal to the surface. XRR data analysis was pursued using Parratt's formalism [47], where the film is assumed to have a stack of multiple homogeneous layers. Surface and interfacial roughnesses have been included in order to analyse the XRR data [48,49]. Electron-density profile (EDP) is extracted from the data fitting, which gives in-plane average electron density (ρ) as a function of depth (z) [48–50]. Surface morphologies of the Glass-Cu-PS films before and after dipping inside the acid solutions were obtained from an atomic force microscopy (NTEGRA Prima, NT-MDT Technology). Semi-contact mode was used for all the scans using silicon cantilever having spring constant of $\approx 11.8 \text{ N m}^{-1}$ [51]. All the scans were performed in a constant force mode over different portions of the films.

3. Results and discussion

XRR profiles (open circles) and the corresponding fitted curves (solid lines) obtained from the Glass-Cu, Glass-Cu-PS3000, Glass-Cu-PS6000 and Glass-Cu-PS9000 films are shown in figure 1a, and the corresponding EDPs are shown in figure 1b. EDPs also show that electron density variation exists along the thickness (z -direction) of the Cu layers. The gradual increase of the PS layer thickness with lowering the spinning speed is also obtained, which is marked by the green line in figure 1b. EDPs show that the thickness of the Cu layer deposited on the glass substrate is $\approx 1024 \text{ \AA}$, whereas on Cu layer, the thicknesses of PS layers are obtained as ≈ 42 , 62 and 147 \AA for 9000, 6000 and 3000 rpm, respectively. The top surface roughness varies from 9 to 15 \AA for thinner to thicker PS films. The X-ray diffraction (XRD) data obtained from the film is shown in figure 1c, where in addition with the amorphous glass peak (obtained at $2\theta \approx 22^\circ$), the Cu fcc (111) peak is visible at $2\theta \approx 43.4^\circ$ from the relatively thick Cu layer [52].

UV-visible absorption spectra obtained from the Glass-Cu-PS3000, Glass-Cu-PS6000 and Glass-Cu-PS9000 films

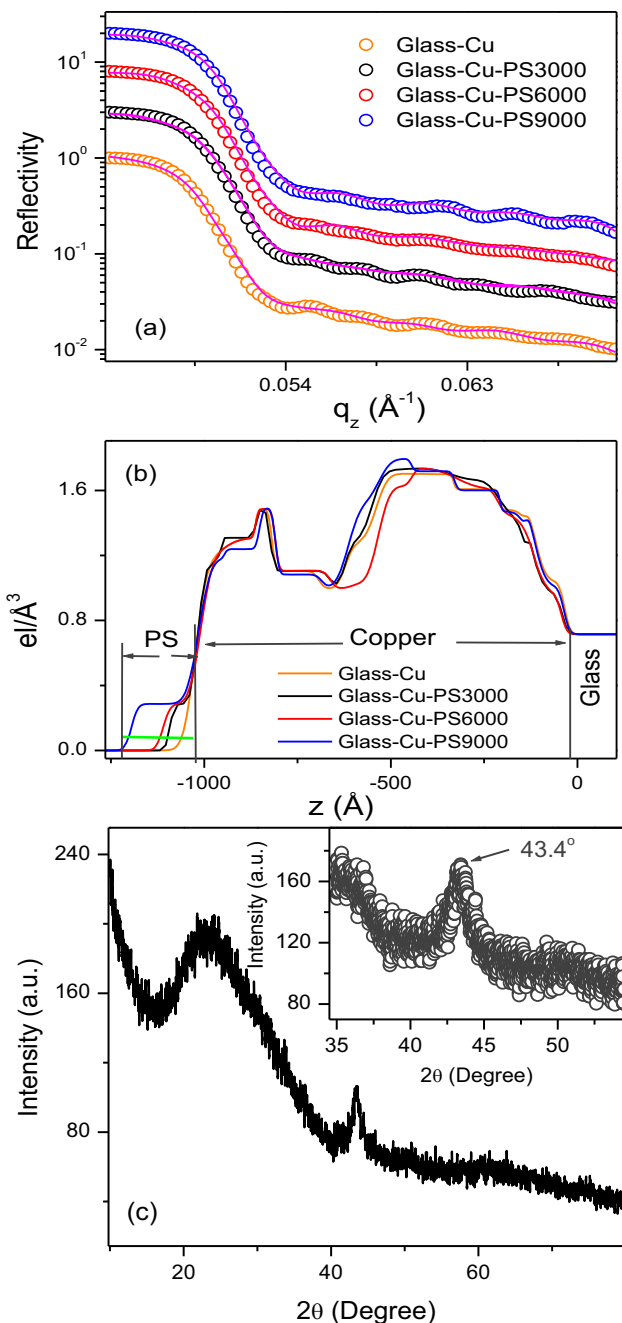


Figure 1. (a) X-ray reflectivity data (open circles) and the corresponding fitted curves (solid lines) obtained from the Glass-Cu, Glass-Cu-PS3000, Glass-Cu-PS6000 and Glass-Cu-PS9000 films. (b) EDPs extracted from the fitting of the reflectivity data of Glass-Cu, Glass-Cu-PS3000, Glass-Cu-PS6000 and Glass-Cu-PS9000 films, respectively. (c) XRD profile obtained from the Glass-Cu film. Inset: zoomed portion around the Cu fcc (111) peak.

with the variation of dipping time inside 1.0, 2.5 and 10.0 vol% acetic acid solutions, respectively, for 120 min are shown in figure 2. In the absorption spectra, a peak is found at $\approx 620 \text{ nm}$ due to thin CuO-coated Cu particles inside the film [53]. It is clear from figure 2a that the

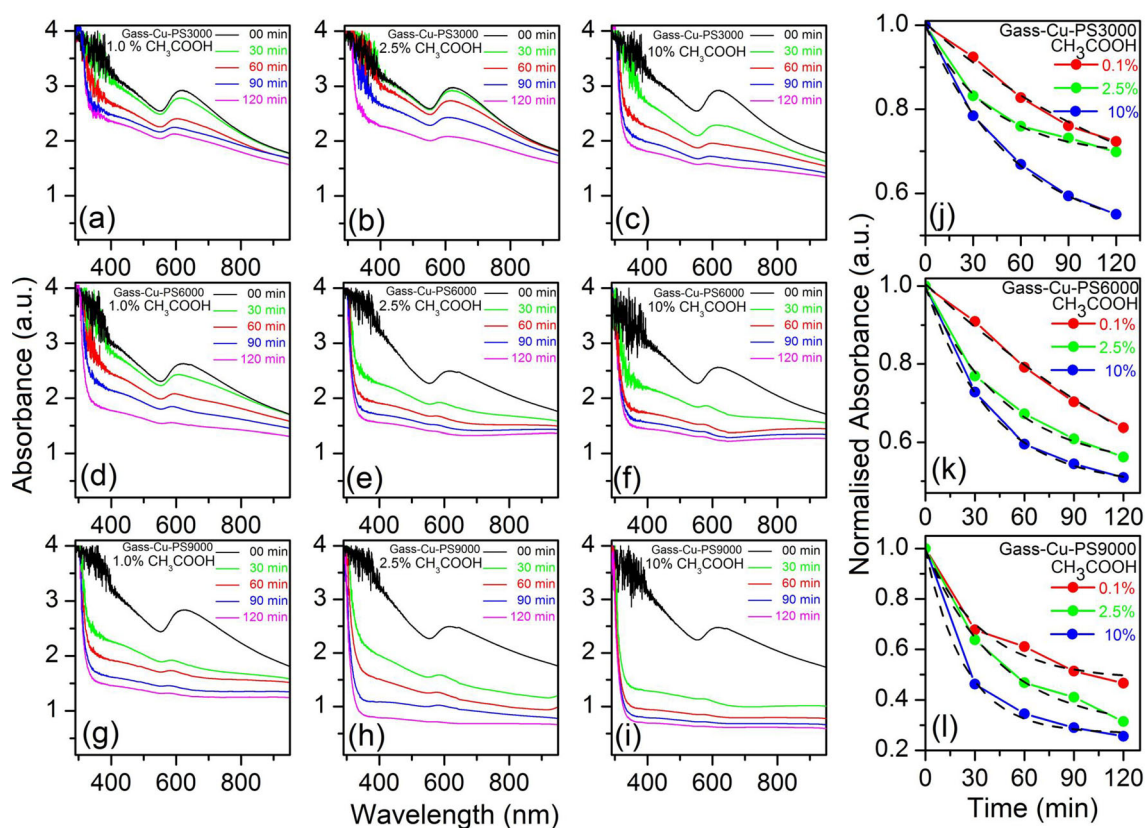


Figure 2. UV–visible absorption spectra obtained from (a–c) Glass-Cu-PS3000, (d–f) Glass-Cu-PS6000 and (g–i) Glass-Cu-PS9000 films for keeping inside acetic acid solutions of concentrations 1, 2.5 and 10 vol% for different time intervals, i.e., for 0 to 120 min. Decay of the normalized absorbance values with time obtained from the (j) Glass-Cu-PS3000, (k) Glass-Cu-PS6000 and (l) Glass-Cu-PS9000 films for dipping inside the acetic acid solutions. Dotted lines are the corresponding exponential decay fits.

initial absorption peak of intensity 2.98 is obtained at ≈ 622 nm.

The peak intensity gradually decreases with increase in dipping time inside the acetic acid solution, and a blue-shift in the peak position is also observed. Due to the penetration of the acid solution through PS coating layer, a reaction occurs between the acid and metallic oxide layer and forms cupric acetate [53], which then comes out from the metal surface into the acid solution. Again with time, oxide layer forms on the newly exposed metal surface, and then again, the reaction occurs with the oxide layer and corrosion takes place. This gradual corrosion reduces the Cu particle size and as a result, blue-shift and decrement in the absorption peak intensity takes place. Thus, gradual decrement in the UV–visible absorption peak can be correlated with the time-dependent corrosion behaviour of the metallic layer. After 30 min, the peak intensity is found to be 2.93 and the peak position is shifted from ≈ 622 to 618 nm; however, after 60, 90 and 120 min the peak intensity becomes 2.73, 2.42 and 2.07, which are found at ≈ 606 , 597 and 592 nm, respectively. Like figure 2a, it is clear from figure 2b–i that the initial absorption peak value gradually decreases with an increase in the dipping time inside acetic acid solutions, and

the peak position is also shifted from the initial value to some lower value depending upon the experimental conditions. Although the same experimental conditions were used but considering all samples, it is found that before dipping, the initial peak position was varied between 624 and 615 nm, and after dipping inside acid solutions, the corresponding peak positions are shifted and found between 619 and 574 nm, respectively. It is also found that for the same acid concentration and dipping time, the decrement of the absorption peak intensity or metallic corrosion is relatively higher for the thinner PS-coated layer, i.e., for the Glass-Cu-PS9000 film.

After normalizing the absorption peak values obtained from each film, the variation of the peak absorptions with time for 1.0, 2.5 and 10.0 vol% acetic acid concentrations are plotted in figure 2j, k and l, respectively. After dipping inside different acetic acid solutions for each sample, the decay plots are fitted using the equation $y(t) = a \cdot \exp(-t/\tau) + y_0$, which is shown by the dotted lines. Among the three constants a , y_0 and τ , the constant τ is the decay time scale. Different τ values obtained from the fitting are shown in table 1. It is clear from the results that the decay rate of absorption or the corrosion of Cu layer

gradually increased from the film Glass-Cu-PS3000 to Glass-Cu-PS9000, as the polymer or coating layer thickness decreases from ≈ 147 to 42 \AA with changing the rotation speed from 3000 to 9000 rpm. This implies that the permeation of the acid solution is dependent on the thickness of the PS coating layer.

UV-visible absorption spectra are also obtained from the Glass-Cu-PS3000, Glass-Cu-PS6000 and Glass-Cu-PS9000 films before and after dipping inside the hydrochloric acid solutions, which are plotted in figure 3. The effect of HCl on the PS-coated Cu films is similar like

the effect of CH_3COOH . However, the difference is found in the dipping period to complete the corrosion process, which is relatively less for HCl than acetic acid. As HCl's strength is much higher than CH_3COOH , therefore, in the presence of HCl, relatively lower acid concentrations, i.e., 0.1, 0.15 and 0.2 vol%, and less dipping time are chosen. In figure 3, UV-visible absorption spectra are plotted for the Glass-Cu-PS3000, Glass-Cu-PS6000 and Glass-Cu-PS9000 films with the variation of dipping time inside 0.1, 0.15 and 0.2 vol% HCl solutions, respectively, for 30 min. In figure 3a, the UV-visible absorption spectra obtained

Table 1. Different τ values obtained from the fitting of the normalized absorbance curves of the three films for different acid conditions.

Acid	Concentration (vol%)	τ values (min) for Glass-Cu-PS3000	τ values (min) for Glass-Cu-PS6000	τ values (min) for Glass-Cu-PS9000
CH_3COOH	1	191.46	72.04	55.82
	2.5	133.22	47.36	39.19
	10	93.71	39.32	23.70
HCl	0.1	12.71	7.41	6.94
	0.15	7.84	5.80	5.74
	0.2	5.23	5.01	4.82

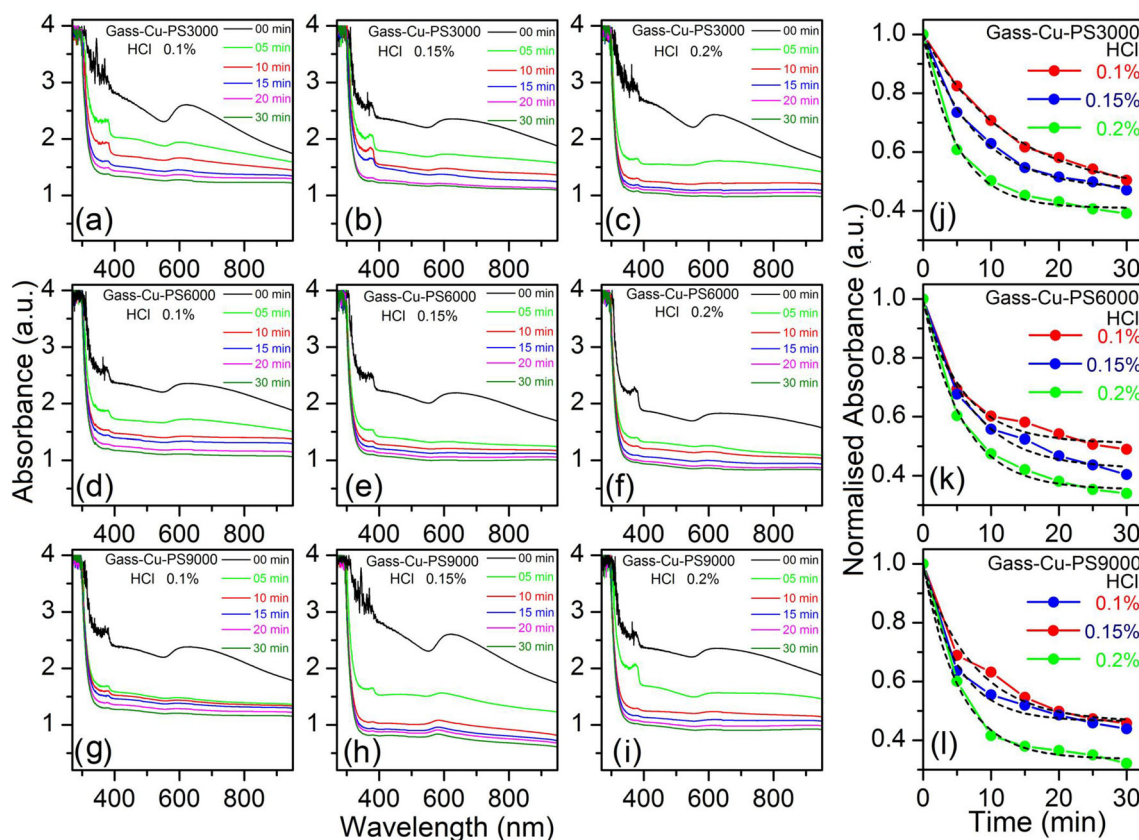


Figure 3. UV-visible absorption spectra obtained from (a–c) Glass-Cu-PS3000, (d–f) Glass-Cu-PS6000 and (g–i) Glass-Cu-PS9000 films, kept inside hydrochloric acid solutions of concentrations 0.1, 0.15 and 0.2 vol% for different time intervals (for 0 to 30 min). Decay of the normalized absorbance values with time obtained from the (j) Glass-Cu-PS3000, (k) Glass-Cu-PS6000 and (l) Glass-Cu-PS9000 films for dipping inside the hydrochloric acid solutions. Dotted lines are the corresponding exponential decay fits.

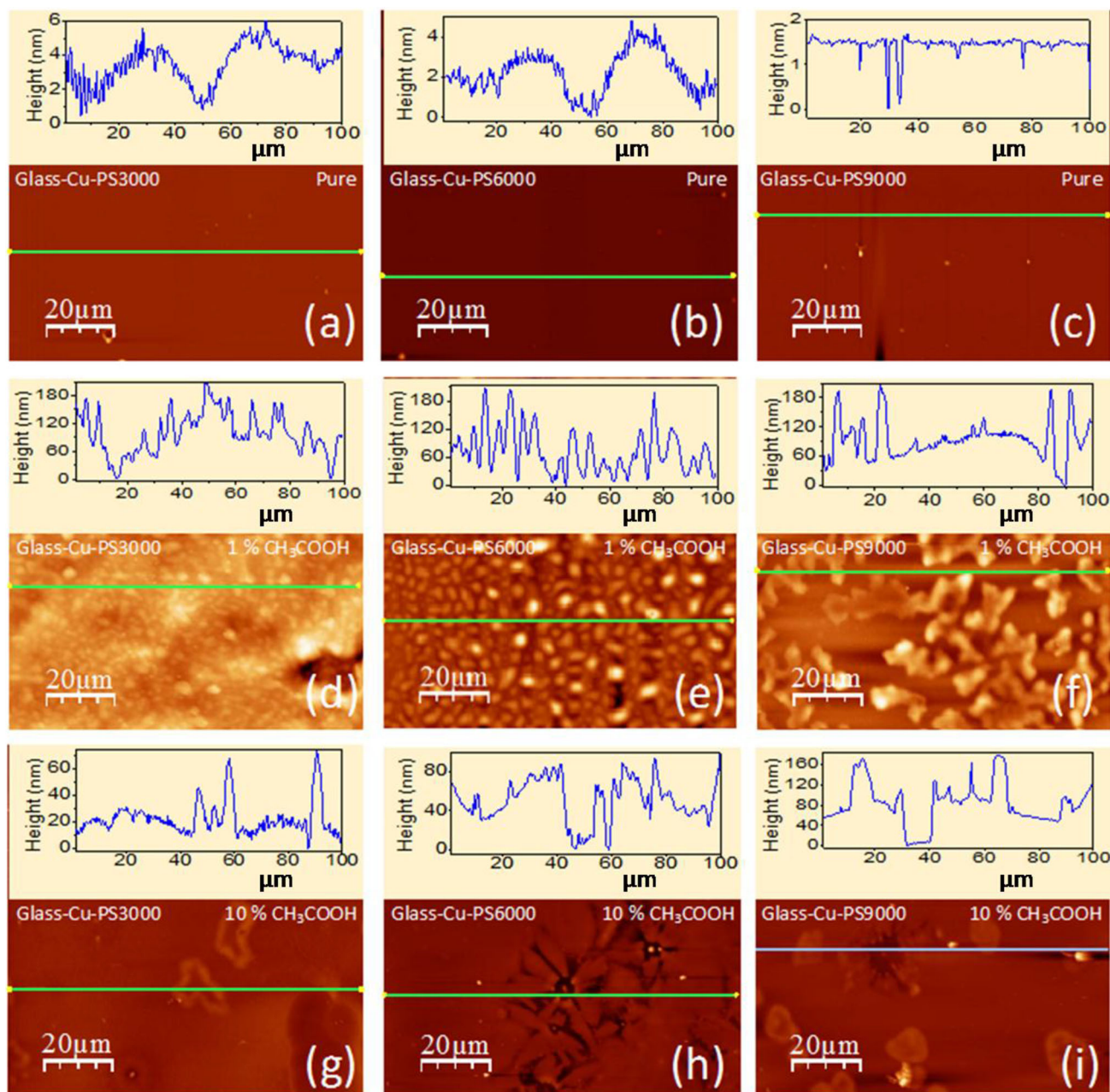


Figure 4. AFM images obtained from the Glass-Cu-PS3000, Glass-Cu-PS6000 and Glass-Cu-PS9000 films (a–c) before and after interaction with the acetic acid solutions of (d–f) 1 and (g–i) 10 vol%, respectively.

from the Glass-Cu-PS3000 film inside 0.1 vol% HCl solution are shown, where the absorption peak of intensity 2.60 is found at ≈ 622 nm, and after interaction with the HCl solution for 5 min the peak is found to be shifted to ≈ 605 nm, and the intensity becomes 1.94. After interaction with the acid solution for 10, 15, 20 and 30 min, the peak intensity becomes 1.66, 1.45, 1.37 and 1.28, and the peak position is shifted to ≈ 602 , 597, 594 and 592 nm, respectively. Like figure 3a, it is clear from figure 3b–i that the initial absorption peak values gradually decreases with increase in the dipping time inside the hydrochloric

acid solutions and the peak positions are also shifted from the initial values to some lower values.

After normalizing the absorption peak values obtained from the films, the variation of the peak absorptions with time for Glass-Cu-PS3000, Glass-Cu-PS6000 and Glass-Cu-PS9000 films after dipping inside hydrochloric acid solutions of 0.1, 0.15 and 0.2 vol% concentrations are shown in figure 3j to l, respectively. For each sample after dipping inside different hydrochloric acid solutions, the decay plots are fitted using the equation $y(t) = a \cdot \exp(-t/\tau) + y_0$, which are shown by the dotted

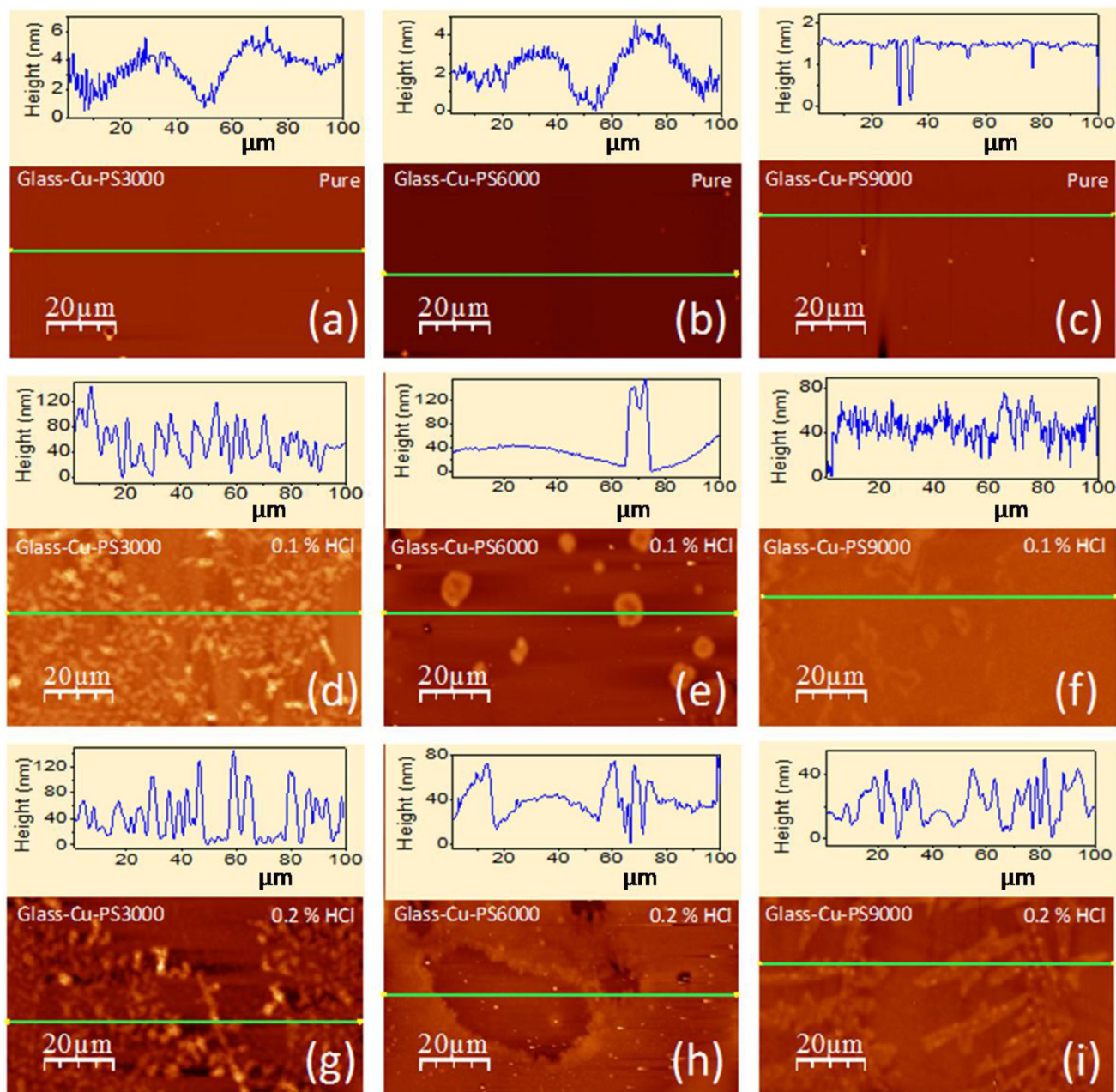


Figure 5. AFM images obtained from the Glass-Cu-PS3000, Glass-Cu-PS6000 and Glass-Cu-PS9000 films (a–c) before and after interaction with the hydrochloric acid solutions of (d–f) 0.1 and (g–i) 0.2 vol%, respectively.

Table 2. RMS roughness values (nm) obtained from the films for different acid conditions.

Acid	Concentration	Glass-Cu-PS3000	Glass-Cu-PS6000	Glass-Cu-PS9000
Pure film		23.70	19.85	8.45
CH ₃ COOH	1 vol%	82.39	77.26	72.43
	10 vol%	20.47	14.70	0.04
HCl	0.1 vol%	72.43	30.68	12.16
	0.2 vol%	32.51	16.92	0.07

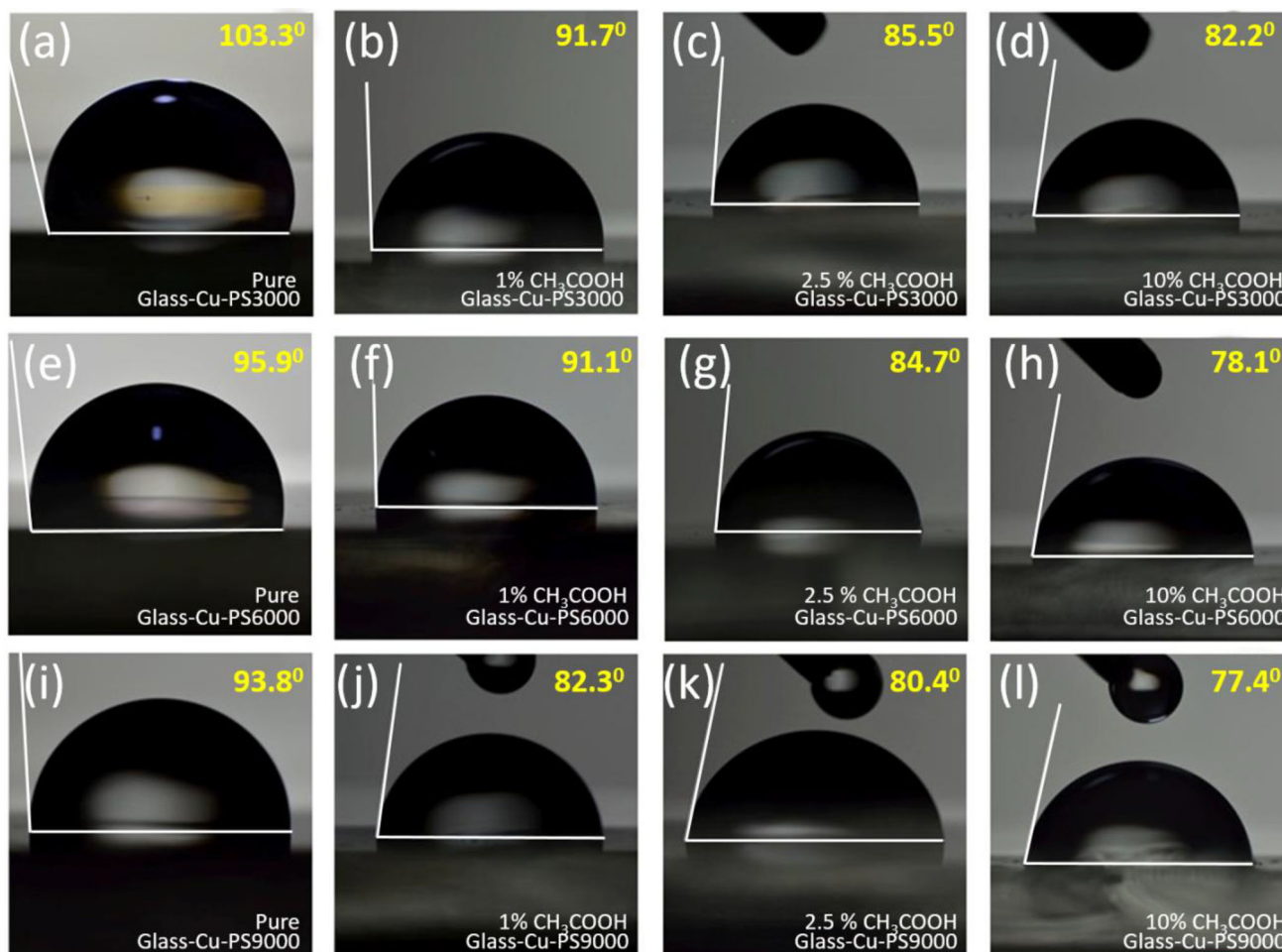


Figure 6. Water contact angles obtained from the Glass-Cu-PS3000 (upper row), Glass-Cu-PS6000 (middle row) and Glass-Cu-PS9000 (lower row) films for different acid conditions; (a, e, i): contact angles from the fresh films. Contact angles after interaction with 1, 2.5 and 10 vol% acetic acid solutions for 120 min from (b–d) Glass-Cu-PS3000, (f–h) Glass-Cu-PS6000 and (j–l) Glass-Cu-PS9000 films, respectively.

lines. Different τ values obtained from the data fitting are shown in table 1. Like before, it is also found from the results that the decay rate of optical absorption is relatively higher for the film for which the PS layer thickness is less.

AFM images depicting the surface morphologies of Glass-Cu-PS3000, Glass-Cu-PS6000 and Glass-Cu-PS9000 films before and after interaction with the acetic and hydrochloric acid solutions of different concentrations are shown in figures 4 and 5, respectively. Figures 4a–c and 5a–c show the surface morphology of the Glass-Cu-PS3000, Glass-Cu-PS6000 and Glass-Cu-PS9000 films, i.e., before treatment with the acids. These films are modified after interaction with the 1 and 10 vol% acetic acid solutions for 120 min and are shown in figure 4d–f and g–i, respectively. Similarly, after interaction with hydrochloric acid for 30 min having a concentration of 0.1 and 0.2 vol%, morphological changes occur on the respective surfaces shown in figure 5d–f and g–i, respectively. It is clear from the images that before interaction with the acids, the film has a smooth

morphology except for some globule-like particles on the surface. After being dipped into the acid solutions, the film morphology gets modified. The modification occurs because the PS-coated Cu layer is partially detached from the glass surface depending on the thickness of the PS coating layer. The height variation for some of the corroded samples is found to be reaching around 200 nm, which is more than the thickness of the films. Probably after interaction with the acidic medium the metallic copper comes out through the organic layer and due to that the outer surface becomes rougher and the thickness of the film also increases in comparison with the thickness of the pure sample. The roughness analysis of the AFM images is based on the standard deviation of all the height values within the given scanned area (rms roughness). The rms values of the Glass-Cu-PS3000, Glass-Cu-PS6000 and Glass-Cu-PS9000 films before and after treatments with both the acids are listed in table 2. There is a significant amount of change in the rms values of the films before and after the acid treatment.

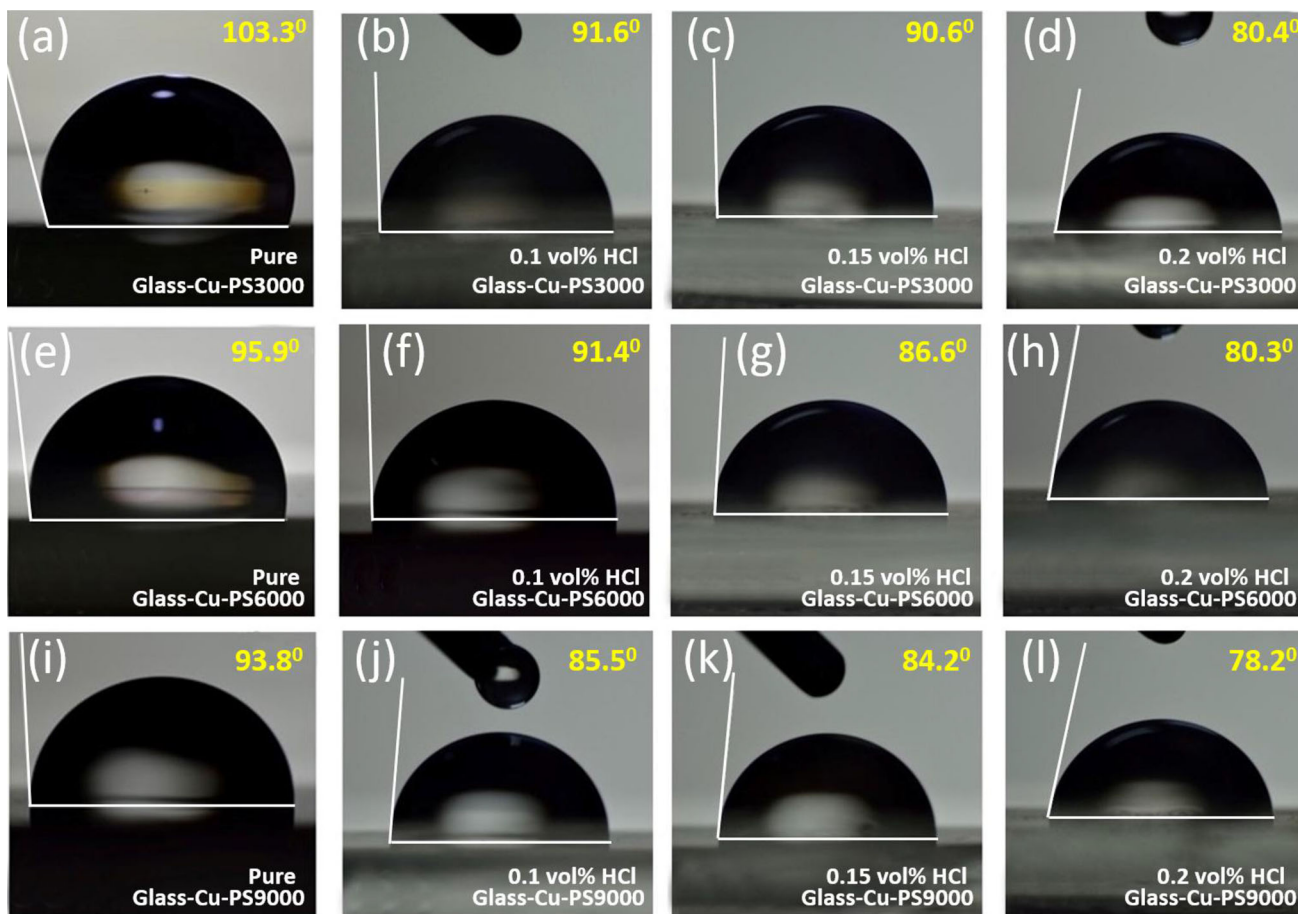


Figure 7. Water contact angles obtained from the Glass-Cu-PS3000 (upper row), Glass-Cu-PS6000 (middle row) and Glass-Cu-PS9000 (lower row) films for different acid conditions. (a, e, i) Contact angles from the fresh films. Different contact angles after interaction with 0.1, 0.15 and 0.2 vol% hydrochloric acid solutions for 30 min from (b–d) Glass-Cu-PS3000, (f–h) Glass-Cu-PS6000 and (j–l) Glass-Cu-PS9000 films, respectively.

For both the acid conditions, the rms values show decrement with decreasing thickness of PS film, while with increase in the acid concentration, the rms values get decreased. It is clear that for the thinnest PS coating layer, i.e., for the Glass-Cu-PS9000 film the gaps between the PS-covered Cu domains on the glass surface are enhanced after acid treatment, which probably reduces the water contact angle values and also the in-plane current.

To compare the modification of hydrophobicity of the films after interaction with the acid media, water contact angle measurements were performed. The data obtained from the PS-coated Cu films before and after dipping inside the acetic and hydrochloric acid solutions are shown in figures 6 and 7, respectively. It is found that the contact angle value of the thicker PS layer (i.e., Glass-Cu-PS3000) is $\approx 103.3^\circ$, which is relatively higher than the value obtained from the thinner one (i.e., Glass-Cu-PS9000) that is $\approx 93.8^\circ$, indicating that the water contact angle or hydrophobicity of the films depends upon the PS layer thickness. Water contact angle value of $\approx 98^\circ$ for PS film is also obtained by another group [54]. However, after the

interaction with the acid solutions, the water contact angle value for each sample decreases. As the PS-coated Cu layer is detached partially from the glass surface after dipping the films inside acid solutions, relatively more glass portions are exposed and therefore contact angle value reduces as the water contact angle of pure glass surface is $\approx 22^\circ$ [55]. It is found that after interaction with 1, 2.5 and 10 vol% CH_3COOH for 120 min, the contact angle of Glass-Cu-PS3000 film reduces to $\approx 91.7^\circ$, 85.5° and 82.2° , respectively, as shown in figure 6b–d. Whereas for Glass-Cu-PS6000 films, the contact angles become $\approx 91.1^\circ$, 84.7° and 78.1° respectively, which are shown in figure 6f–h and for Glass-Cu-PS9000 films, the contact angle values are found to be $\approx 82.3^\circ$, 80.4° and 77.4° after interaction with 1, 2.5 and 10 vol% acetic acid solutions for 120 min as shown in figure 6j–l.

Similar results are also obtained for HCl solutions. In figure 7a–c, images of the water contact angles of the fresh Glass-Cu-PS3000, Glass-Cu-PS6000 and Glass-Cu-PS9000 samples are shown with the corresponding contact angle values of $\approx 103.3^\circ$, 95.9° and 93.8° , respectively.

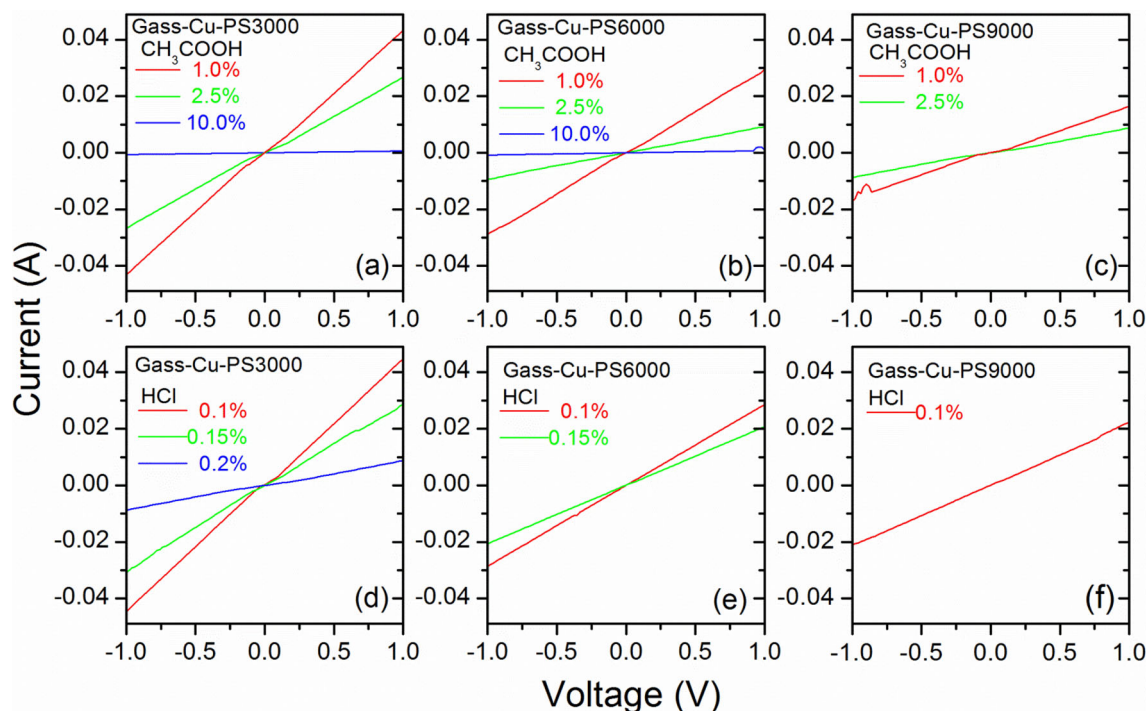


Figure 8. Current–voltage (I – V) characteristics obtained from (a) Glass-Cu-PS3000, (b) Glass-Cu-PS6000 and (c) Glass-Cu-PS9000 films after dipping inside 1.0, 2.5 and 10 vol% acidic acid, and (d) Glass-Cu-PS3000, (e) Glass-Cu-PS6000 and (f) Glass-Cu-PS9000 films after dipping inside 0.1, 0.15 and 0.2 vol% hydrochloric acid solutions, respectively.

Figure 7b–d shows the water contact angles of Glass-Cu-PS3000 films after interaction with 0.1, 0.15 and 0.2 vol% HCl solutions for 30 min and it shows that like acetic acid the hydrophobicity of these films also decreases and the contact angles become $\approx 91.6^\circ$, 90.6° and 80.4° , respectively. After interaction with 0.1, 0.15 and 0.2 vol% HCl solutions for 30 min, the contact angle values for Glass-Cu-PS6000 films are found to be $\approx 91.4^\circ$, 86.6° and 80.3° , respectively, as shown in figure 7f–h, while for Glass-Cu-PS9000 films the contact angle reduces to $\approx 85.5^\circ$, 84.2° and 78.2° , respectively, as shown in figure 7j–l. Results obtained from the experiments show that for each film, the contact angle value reduces if the acid concentration is increased. Contact angle values also show that the PS layer is partially detached from the film surface.

It is obvious that due to the interaction with the acid solutions, the metallic layer of the films will be eroded and due to that the in-plane electrical behaviours will be modified. Therefore, electrical measurements are performed on all the films after dipping inside acid solutions. The current–voltage (I – V) characteristics of all the films before and after dipping inside the acetic and hydrochloric acid solutions are shown in figure 8a–c and d–f, respectively. For 1.0 V of applied voltage, the value of the current obtained from the Cu/Glass film is ≈ 0.104 A. However, before dipping, all three Glass-Cu-PS3000, Glass-Cu-PS6000 and Glass-Cu-PS9000 films behave like an insulator, as a non-conducting PS layer was present over the Cu surface. Figure 8 shows

the I – V characteristics obtained from all the three films after dipping inside the acetic acid for 120 min and hydrochloric acid for 30 min, which are actually Ohmic in nature. In figure 8a–c, the I – V curves of Glass-Cu-PS3000, Glass-Cu-PS6000 and Glass-Cu-PS9000 films are shown after interaction with 1 (red), 2.5 (green) and 10 vol% (blue) acetic acid solutions, respectively. For Glass-Cu-PS3000 film, the maximum values of currents obtained for 1.0 V of applied voltage in three different acid concentrations are ≈ 43.2 , 26.7 and 8.7 mA, respectively, shown in figure 8a. In figure 8b, the maximum values of currents for Glass-Cu-PS6000 film after interaction with the three different acid concentrations are shown, which are obtained as ≈ 29.5 , 9.7 and 5.7 mA, respectively. However, for Glass-Cu-PS9000 film, after interaction with the three different acid concentrations the currents obtained are ≈ 16.4 and 9.2 mA for 1 and 2.5 vol%, respectively. For 10 vol% solution, the film becomes insulator due to the major removal of the metallic layer after dipping inside the relatively stronger acid solution and also for the thinner coating layer of PS, which is shown in figure 8c. As the metallic layer is gradually eroded after interaction with the acid solutions, the in-plane connectivity decreases due to the formation of voids or defects inside metallic layer, which reduces the in-plane current and indirectly gives the information of metallic corrosion.

Similarly, the I – V characteristics of Glass-Cu-PS3000, Glass-Cu-PS6000 and Glass-Cu-PS9000 films after dipping inside the different concentrations of HCl solutions for 30

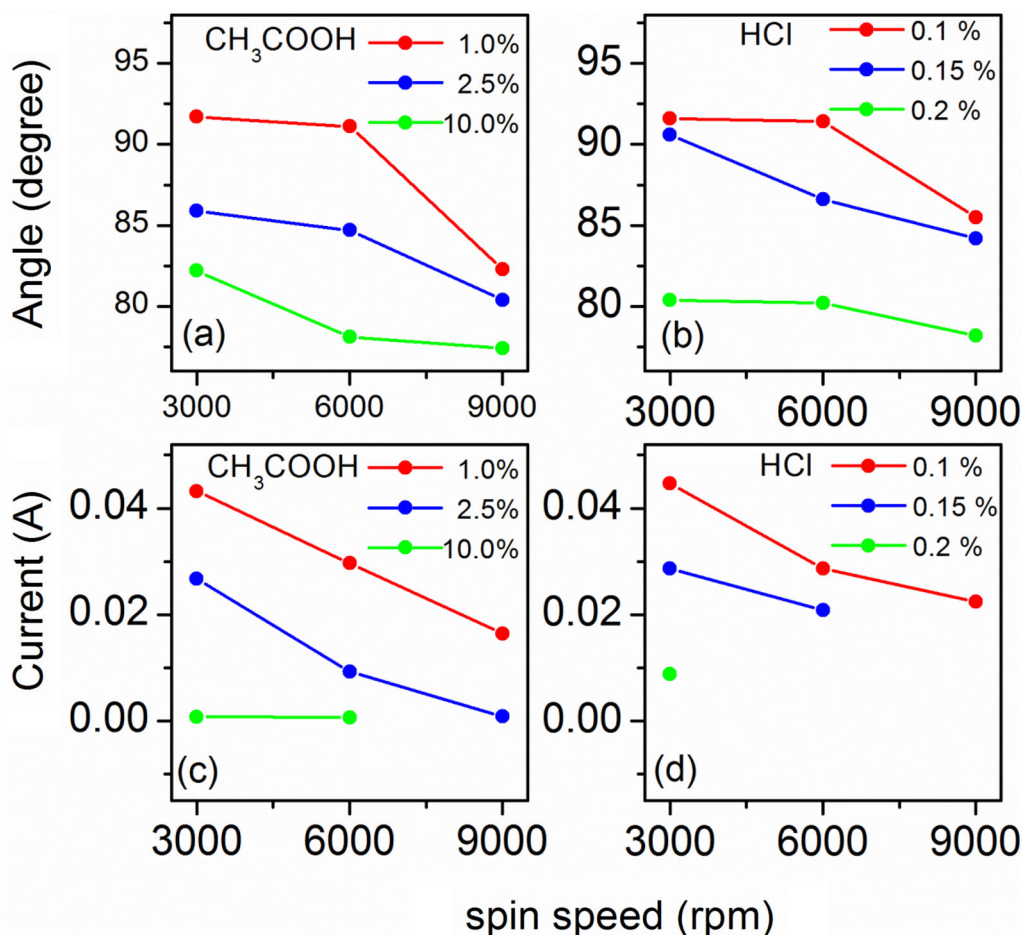


Figure 9. Plots of the water contact angles of Glass-Cu-PS3000, Glass-Cu-PS6000 and Glass-Cu-PS9000 films after dipping inside (a) acetic acid (1, 2.5, 10 vol%) and (b) hydrochloric acid (0.1, 0.15 and 0.2 vol%) solutions, respectively. Plots of currents obtained from *I*–*V* characteristics of Glass-Cu-PS3000, Glass-Cu-PS6000 and Glass-Cu-PS9000 films after dipping inside (c) acetic acid (1, 2.5, 10 vol%) and (d) hydrochloric acid (0.1, 0.15 and 0.2 vol%) solutions, respectively.

min are shown in figure 8d–f. The red, blue and green lines indicate the variation of current with the applying voltage (for 1.0 V) for each film after interaction with 0.1, 0.15, and 0.2 vol% HCl solutions and the values of currents obtained are ≈44.6, 28.6 and 8.7 mA, respectively, which is shown in figure 8d. In figure 8e, *I*–*V* characteristics of Glass-Cu-PS6000 films are shown where the currents (for 1.0 V) of ≈28.5 and 20.7 mA are obtained for lower and medium HCl concentrations, respectively; as for the higher concentration of HCl, the corrosion of metallic layer is more. For the Glass-Cu-PS9000 film, the current of ≈22.4 mA is obtained only from the 0.1 vol% HCl solution, which is shown in figure 8f; as for the other two acid concentrations, the in-plane electrical connectivity was very less.

Results obtained from the UV–visible study clearly confirm that although PS working as a weak coating layer but for such dilute acid concentrations, the corrosion of the metallic layer nearly follows the exponential decay nature with time. The decay time constant (τ) varies with different

experimental conditions. For the thicker PS coating layer, the corrosion of metal is relatively less than the thinner coating layer and therefore, the τ value is lower for the films for which PS layer thickness is less. In addition, for a particular thickness of the coating layer, the amount of corrosion depends upon the acid concentration also and accordingly the τ value also changes. To compare the surface hydrophobicity/hydrophilicity and metallic layer connectivity, the water contact angles and in-plane currents (for constant voltage of 1.0 V) obtained from the films after dipping inside the acetic and hydrochloric acid solutions are plotted in figure 9a, b and c, d, respectively, as a function of rpm used for PS film deposition (i.e., film thickness variation).

It is clear that for a particular acid concentration, the contact angle, i.e., film hydrophobicity and the in-plane current, decreases with the decrease in film thickness. Thus, both the organic and metallic layers are partially removed in the acidic medium, but the corrosion of the metallic layer is much more than the organic layer. For example, at 1 vol%

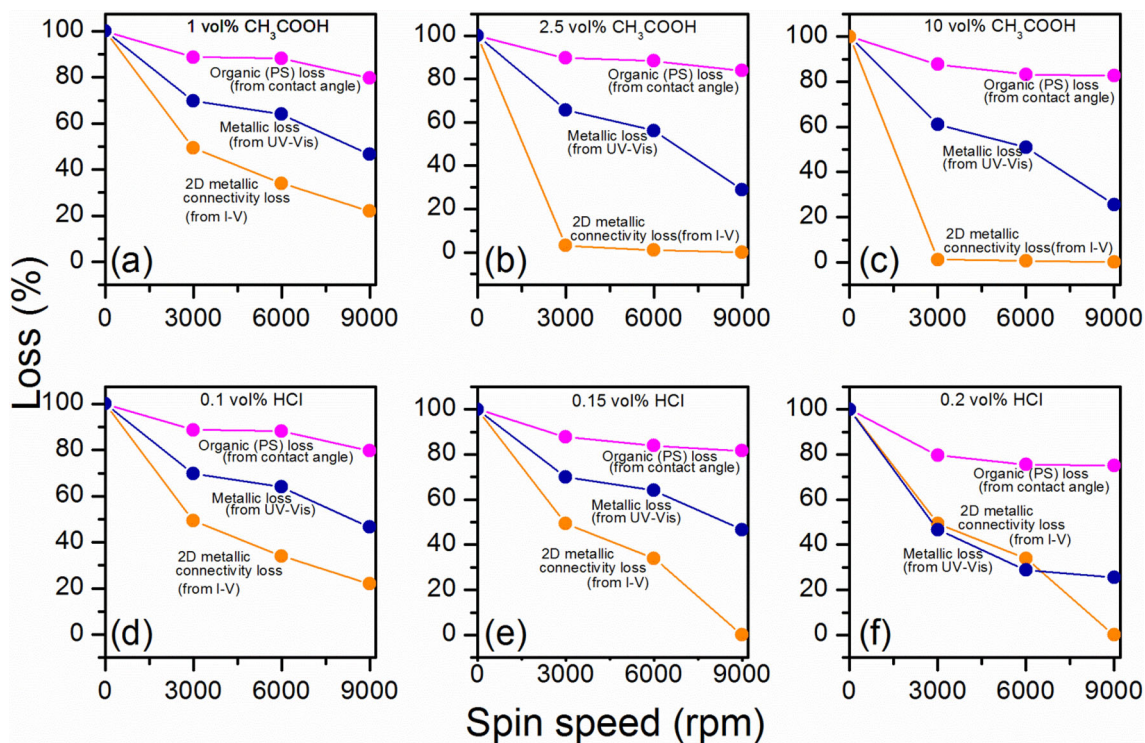


Figure 10. The variation of polymeric and metallic materials loss after dipping inside the acetic acid solutions of (a) 1.0, (b) 2.5 and (c) 10.0 vol%, and hydrochloric acid solutions of (d) 0.1, (e) 0.15 and (f) 0.2 vol%, respectively. Comparison is made considering the information obtained from the water contact angle, UV-Vis and *I-V* analysis.

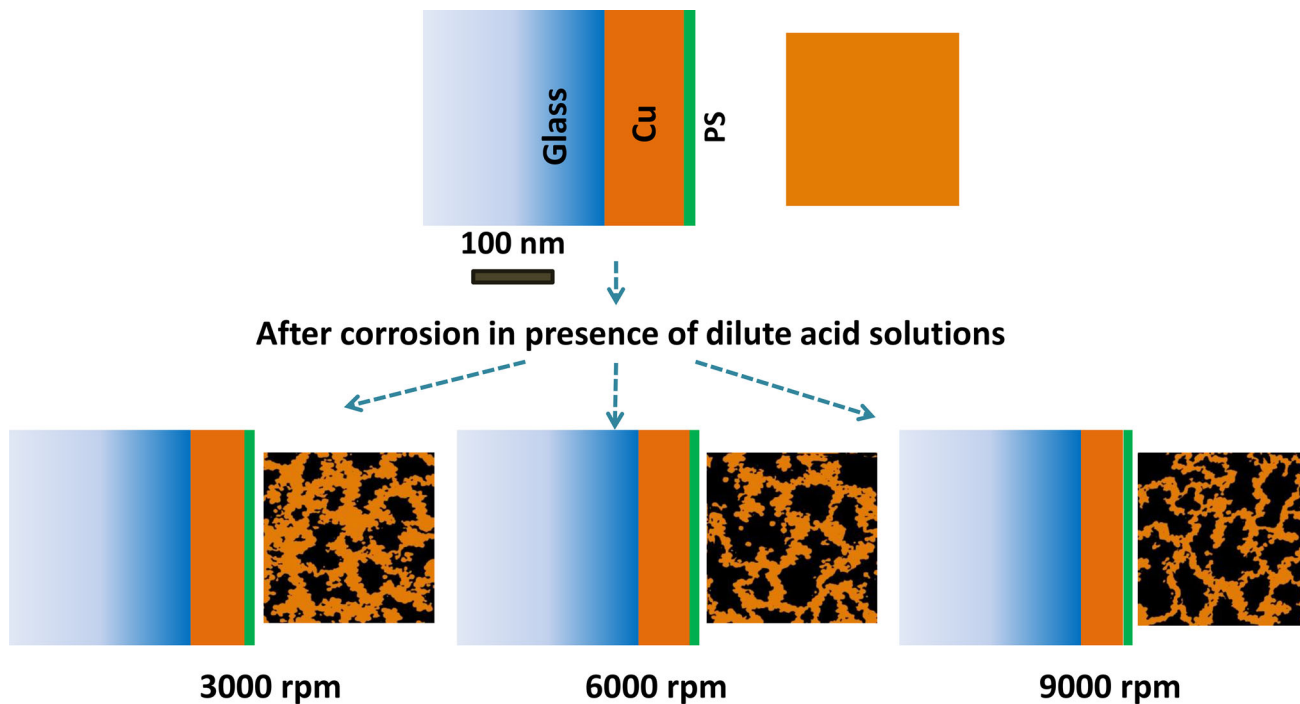


Figure 11. Schematic representation of the variation of both organic (PS) and metallic (Cu) materials due to corrosion, where total loss of materials are shown as out-of-plane or cross-sectional view, whereas 2D metallic connectivity loss is shown as in-plane view. Scale bar is for the cross-sectional view only.

acetic acid concentration, due to corrosion, the PS layer is reduced by 11.2, 10.8 and 12.4% from its initial value for three different PS layer thicknesses, as obtained from the contact angle modification. However, for the same acid concentration and for the three different coating layer thicknesses, the metallic layer is reduced by 30.2, 35.9 and 53.4% from its initial value, and the corresponding 2D metallic connectivity is reduced by 50.1, 68.1 and 75.0% as obtained from the UV-visible and $I-V$ measurements, respectively. The variations of losses of the organic and metallic materials due to corrosion are shown in figure 10a, b, c and d, e, f for both acetic and hydrochloric acids, respectively. The variations of losses of both organic (PS) and metallic (Cu) materials are also shown schematically in figure 11, where total loss of materials are shown as out-of-plane or cross-sectional view, whereas 2D metallic connectivity loss is shown as in-plane view. Most probably, the lower thickness of PS helps the acid solutions to penetrate the coating barrier relatively more easily through intermolecular spacing or microscopic pores of the organic layer and as a result film modification or metallic layer corrosion takes place. However, the hydrophobic polymeric layer mostly stays attached to the solid surface as dissolving into the aqueous acid solutions are not energetically favourable. Thus, our study shows the morphological modification of the PS-coated Cu layer inside acid solutions and confirms that the metallic layer corrosion in the presence of the polymeric coating layer follows exponential decay with dipping time. Again, for dilute acid condition, the metallic layer corrosion is much more than the corrosion of the organic coating layer.

4. Conclusions

Surface modification of the PS thin film-coated Cu layer and the corrosion of both the metallic and polymeric layers are studied by varying the thickness of PS layer and acid concentration. PS and Cu layers are formed by using spin coating and DC magnetron sputtering methods, respectively. Thicknesses of both the PS and Cu layers are obtained analysing the X-ray reflectivity data, whereas the surface morphology and nature of corrosion of the PS-coated Cu layers dipped inside different acid solutions are studied using UV-visible spectroscopy, AFM, water contact angle and in-plane $I-V$ characteristics. The variation of the absorption peak value with time as obtained from the UV-visible spectra confirms the exponential decay nature of metallic layer corrosion with dipping time and it is found that the decay time constant (τ) takes the higher values for the thicker PS films. AFM provides the morphological modifications or voids formation after corrosion, while contact angle and in-plane current measurements show that the PS-covered Cu layer is partially removed. However, the corrosion of the metallic layer is much more than the polymeric layer. Penetration of acid solutions through the

intermolecular spacing or microscopic pores of the organic layer is the most probable reason for such metallic corrosion. However, the removal of the polymeric layer is relatively very less as is not favourable due to hydrophobic effect.

Acknowledgements

This study was supported by Department of Science and Technology (DST), Ministry of Science, Govt. of India. SS and BKS acknowledge the Council for Scientific and Industrial Research (CSIR), Govt. of India, for CSIR-SRF fellowship.

References

- [1] Yao C W, Sebastian D, Lian I, Günaydın-Şen Ö, Clarke R, Clayton K *et al* 2018 *Coatings* **8** 10
- [2] Es-Saheb M, Sayed E, Sherif M, El-zatahry A, Rayes M M E and Khalil K A 2012 *Int. J. Electrochem. Sci.* **7** 10442
- [3] Li G, Yue J, Guo C and Ji Y 2018 *Constr. Build. Mater.* **169** 1
- [4] Li G, Guo C, Gao X, Ji Y and Geng O 2016 *Constr. Build. Mater.* **114** 269
- [5] Románszki L, Datsenko I, May Z, Telegdi J, Nyikos L and Sand W 2014 *Bioelectrochemistry* **97** 7
- [6] Laibinis P E and Whitesides G M 1992 *J. Am. Chem. Soc.* **114** 9022
- [7] Yamamoto Y 1993 *J. Electrochem. Soc.* **140** 436
- [8] Kane Jennings G and Laibinis Paul E 1998 *Org. Coatings Corros. Control.* **689** 409
- [9] Aramaki K 1999 *Corros. Sci.* **41** 1715
- [10] Mekhalif Z, Sinapi F, Laffineur F and Delhalle J 2001 *J. Electron. Spectros. Relat. Phenomena* **121** 161
- [11] Ruan C, Bayer T, Meth S and Sukenik C N 2002 *Thin Solid Films* **419** 95
- [12] Ma H Y, Yang C, Yin B S, Li G Y, Chen S H and Luo J L 2003 *Appl. Surf. Sci.* **218** 143
- [13] Whelan C M, Kinsella M, Carbonell L, Ho H M and Maex K 2003 *Microelectron. Eng.* **70** 551
- [14] Sinapi F, Deroubaix S, Pirlot C, Delhalle J and Mekhalif Z 2004 *Electrochim. Acta* **49** 2987
- [15] Tan Y S, Srinivasan M P, Pehkonen S O and Chooi S Y M 2004 *J. Vac. Sci. Technol. A* **22** 1917
- [16] Hutt D A and Liu C 2005 *Appl. Surf. Sci.* **252** 400
- [17] Zhang H, Romero C and Baldelli S 2005 *J. Phys. Chem. B* **109** 15520
- [18] Tan Y S, Srinivasan M P, Pehkonen S O and Chooi S Y M 2006 *Corros. Sci.* **48** 840
- [19] Hao C, Yin R H, Wan Z Y, Xu Q J and Zhou G D 2008 *Corros. Sci.* **50** 3527
- [20] Hong Y, Patri U B, Ramakrishnan S, Roy D and Babu S V 2005 *J. Mater. Res.* **20** 3413
- [21] Lusk A T and Jennings G K 2001 *Langmuir* **17** 7830
- [22] Tao Y T, Hietpas G D and Allara D L 1996 *J. Am. Chem. Soc.* **118** 6724

- [23] Aramaki K and Shimura T 2004 *Corros. Sci.* **46** 313
- [24] Li D, Chen S, Zhao S and Ma H 2006 *Colloids Surf. A Physicochem. Eng. Asp.* **273** 16
- [25] Raman A and Gawalt E S 2007 *Langmuir* **23** 2284
- [26] Sahoo R R and Biswas S K 2009 *J. Colloid Interface Sci.* **333** 707
- [27] Ghareba S and Omanovic S 2010 *Corros. Sci.* **52** 2104
- [28] Raman A, Quiñones R, Barriger L, Eastman R, Parsi A and Gawalt E S 2010 *Langmuir* **26** 1747
- [29] Alagta A, Felhősi I, Bertoti I and Kálmán E 2008 *Corros. Sci.* **50** 1644
- [30] Deng H, Nanjo H, Qian P, Xia Z, Ishikawa I and Suzuki T M 2008 *Electrochim. Acta* **53** 2972
- [31] Zhang D Q, He X M, Cai Q R, Gao L X and Kim G S 2009 *J. Appl. Electrochem.* **39** 1193
- [32] Zhang D Q, Gao L X, Cai Q R and Lee K Y 2010 *Mater. Corros.* **61** 16
- [33] Zhang D Q, He X M, Cai Q R, Gao L X and Kim G S 2010 *Thin Solid Films* **518** 2745
- [34] Hoque E, DeRose J A, Bhushan B and Hips K W 2009 *Ultramicroscopy* **109** 1015
- [35] Kahyarian A, Schumaker A, Brown B and Nestic S 2017 *Electrochim. Acta* **258** 639
- [36] Singh V B and Singh R N 1995 *Corros. Sci.* **37** 1399
- [37] Maeng W Y and Macdonald D D 2008 *Corros. Sci.* **50** 2239
- [38] Levin M, Wiklund P and Leygraf C 2012 *Corros. Sci.* **58** 104
- [39] Abdallah M, Sobhi M and Altass H M 2016 *J. Mol. Liq.* **223** 1143
- [40] Abdel-Rehim S S, Khaled K F and Al-Mobarak N A 2011 *J. Chem.* **4** 333
- [41] Li G, Yang B, Guo C, Du J and Wu X 2015 *Constr. Build. Mater.* **83** 19
- [42] Khanzadeh Moradllo M, Shekarchi M and Hoseini M 2012 *Constr. Build. Mater.* **30** 198
- [43] Khanzadeh Moradllo M, Sudbrink B and Ley M T 2016 *Constr. Build. Mater.* **116** 121
- [44] Szabó T, Molnár-Nagy L, Bognár J, Nyikos L and Telegdi J 2011 *Prog. Org. Coatings* **72** 52
- [45] Lisiecki I and Pileni M P 1995 *J. Phys. Chem.* **99** 5077
- [46] Talukdar H and Kundu S 2017 *J. Mol. Struct.* **1143** 84
- [47] Parratt L G 1954 *Phys. Rev.* **95** 359
- [48] Daillant J and Gibaud A 1999 (eds) *X-ray and neutron reflectivity: principles and applications* (Springer: Berlin)
- [49] Tolan M 1999 (eds) *Reflectivity of X-rays from surfaces* (Berlin: Springer)
- [50] Das K and Kundu S 2016 *Colloids Surf. A: Physicochem. Eng. Asp.* **492** 54
- [51] Bhowal A C and Kundu S 2016 *J. Mol. Liq.* **224** 89
- [52] Park B K, Jeong S, Kim D, Moon J, Lim S and Kim J S 2007 *J. Colloid Interface Sci.* **311** 417
- [53] Chan G H, Zhao J, Hicks E M, Schatz G C and Van Duyne R P 2007 *Nano Lett.* **7** 1947
- [54] Yuan Z, Chen H, Tang J, Gong H, Liu Y, Wang Z *et al* 2007 *J. Phys. D: Appl. Phys.* **40** 3485
- [55] Ozkan O and Erbil H Y 2017 *Surf. Topogr.: Metrol. Prop.* **5** 024002